

AD-A043 182

HARVARD COLL OBSERVATORY CAMBRIDGE MASS CENTER FOR AS--ETC F/G 3/2
EUV ANALYSIS OF POLAR PLUMES, (U)

AUG 77 I A AHMAD, G L WITHBROE

F19628-76-C-0281

UNCLASSIFIED

PREPRINT-734

AFGL-TR-77-0167

NL

| OF |
ADA043182



END
DATE
FILMED
9-77
DDC

AFGL-TR 77-0167

13
P.S.

CENTER FOR ASTROPHYSICS

PREPRINT SERIES

No. 734

EUV ANALYSIS OF POLAR PLUMES

Imad A. Ahmad and George L. Withbroe

DISTRIBUTION STATEMENT A
Approved for public release;
Distribution Unlimited

DDC
RECEIVED
AUG 19 1977
RECEIVED
B

Accepted for publication
Solar Physics
In press (1977)

Center for Astrophysics
60 Garden St.
Cambridge, Massachusetts 02138

Harvard College Observatory

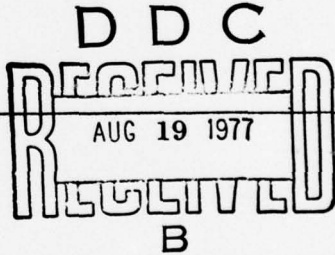
✓ Smithsonian Astrophysical Observatory

AD A U 43182

AD No.
DDC FILE COPY

Unclassified

SECURITY CLASSIFICATION OF THIS PAGE (When Data Entered)

REPORT DOCUMENTATION PAGE		READ INSTRUCTIONS BEFORE COMPLETING FORM
1. REPORT NUMBER AFGL-TR-77-0167	2. GOVT ACCESSION NO.	3. RECIPIENT'S CATALOG NUMBER
4. TITLE (and Subtitle) EUV ANALYSIS OF POLAR PLUMES		5. TYPE OF REPORT & PERIOD COVERED Scientific Report No. 1 (Reprint)
		6. PERFORMING ORG. REPORT NUMBER
7. AUTHOR(s) Imad A. Ahmad George L. Withbroe		8. CONTRACT OR GRANT NUMBER(s) F19628-76-C-0281 <i>New</i>
9. PERFORMING ORGANIZATION NAME AND ADDRESS Smithsonian Institution 60 Garden Street Cambridge, MA 02138		10. PROGRAM ELEMENT, PROJECT, TASK AREA & WORK UNIT NUMBERS 62101F 46430302
11. CONTROLLING OFFICE NAME AND ADDRESS Air Force Geophysics Laboratory Hanscom AFB, Massachusetts 01731 Monitor/Ronald M. Straka/PHP		12. REPORT DATE 3 August 1977
		13. NUMBER OF PAGES 23
14. MONITORING AGENCY NAME & ADDRESS (if different from Controlling Office)		15. SECURITY CLASS. (of this report) Unclassified
		15a. DECLASSIFICATION/DOWNGRADING SCHEDULE
16. DISTRIBUTION STATEMENT (of this Report) Approved for public release; distribution unlimited.		
17. DISTRIBUTION STATEMENT (of the abstract entered in Block 20, if different from Report)		
18. SUPPLEMENTARY NOTES Accepted for publication, Solar Physics (1977)		
19. KEY WORDS (Continue on reverse side if necessary and identify by block number) EUV Polar plumes Density gradients Coronal holes		
20. ABSTRACT (Continue on reverse side if necessary and identify by block number) Three polar plumes were studied using Skylab Mg X and O VI data. The plumes lie within the boundaries of a polar coronal hole. We find that the mean temperature of the plumes is about 1.1×10^6 K and that they have a small vertical temperature gradient. Densities are determined and found consistent with white light analyses. The variation of density with height in the plumes is compared with that expected for hydrostatic equilibrium. As is the case for other coronal features, polar plumes will be a source of solar wind if the magnetic field lines are open. On the basis of the derived plume model and estimates of		

Unclassified

SECURITY CLASSIFICATION OF THIS PAGE (When Data Entered)

the numbers of plumes in polar coronal holes, it appears that polar plumes contain about 15% of the mass in a typical polar hole and occupy about 10% of the volume.

Unclassified

SECURITY CLASSIFICATION OF THIS PAGE (When Data Entered)

18 AFGL-TR-77-0167

14 Center for Astrophysics
Preprint ~~Series No.~~ 734, Scientific-1

6 EUV ANALYSIS OF POLAR PLUMES

10 Imad A. Ahmad and George L. Withbroe
Center for Astrophysics

Harvard College Observatory and Smithsonian Astrophysical Observatory
Cambridge, Massachusetts 02138

11 3 Aug 77 12 26p.

15 F19628-76-C-0281

16 4643

12 03

ACCESSION for	
NTIS	Web Section <input checked="" type="checkbox"/>
DDC	B Section <input type="checkbox"/>
UNANNOUNCED	<input type="checkbox"/>
JUSTIFICATION	
BY	
DISTRIBUTION/AVAILABILITY CODES	
Dist.	and/or SPECIAL
A	

409 956

mt

EUV ANALYSIS OF POLAR PLUMES

IMAD A. AHMAD*

and

GEORGE L. WITHBROE

Center for Astrophysics

Harvard College Observatory and

Smithsonian Astrophysical Observatory

Cambridge, Massachusetts 02138

ABSTRACT

Three polar plumes were studied using Skylab Mg X and O VI data. The plumes lie within the boundaries of a polar coronal hole. We find that the mean temperature of the plumes is about 1.1×10^6 K and that they have a small vertical temperature gradient. Densities are determined and found consistent with white light analyses. The variation of density with height in the plumes is compared with that expected for hydrostatic equilibrium. As is the case for other coronal features, polar plumes will be a source of solar wind if the magnetic field lines are open. On the basis of the derived plume model and estimates of the numbers of plumes in polar coronal holes, it appears that polar plumes contain about 15% of the mass in a typical polar hole and occupy about 10% of the volume.

*Skylab Solar Workshop post-doc appointee 1975-1976. (Present address: American Science and Engineering, Cambridge, Mass.) The Skylab Solar Workshops are sponsored by NASA and NSF and managed by the High Altitude Observatory, National Center for Atmospheric Research.

1. Introduction

Polar plumes, which are believed to trace open magnetic field lines at the solar poles, have been intensively analyzed using white light eclipse photographs (cf. Van de Hulst, 1950; Nikolsky, 1956; Dziubenko, 1957; Saito, 1958, 1965; Newkirk and Harvey, 1968). These features have also been observed in extreme ultraviolet (EUV) emission lines by the Naval Research Laboratories (NRL) and Harvard experiments on Skylab (cf. Bohlin, et al., 1975a, 1975b; Ahmad, 1976). Bohlin et al. (1975a, 1975b) concluded that EUV polar plumes are the EUV counterparts of white light plumes because of their similar temperatures, density gradients, sizes and orientations. The results of Bohlin, et al., are based on the analysis of photographic observations acquired by the NRL Skylab experiment. Temperatures were inferred from the presence or absence of plumes in spectroheliograms of emission lines in the spectral region 250 - 610Å. Density gradients were derived from Mg IX λ 368 intensities.

The present paper reports results of an analysis of Mg X λ 625 and O VI λ 1032 observations of polar plumes obtained by the Harvard Skylab experiment. This experiment, which employed a photoelectric detection system, provided photometrically calibrated measurements with a spatial resolution of 5 arc sec x 5 arc sec (cf. Reeves, et al., 1977). These data have been utilized to derive temperature-density models for three polar plumes.

Determination of the physical conditions in polar plumes is important because these features are a major contributor to the XUV, white light and radio emission from polar coronal holes. Knowledge of the physical conditions in polar coronal holes and features such as polar plumes, which are contained in these areas, is critical to

the development of theories accounting for the association of high speed solar wind streams with coronal holes (cf. Krieger, et al., 1974; Neupert and Pizzo, 1974; Bell and Noci, 1976; Nolte, et al. 1976; Sheeley, et al., 1976). Because polar plumes appear to be associated with open field lines, they may contribute a significant amount of material to the solar wind originating from polar coronal holes.

2. Observations

As indicated above, polar plumes are observed at the solar poles in regions of low coronal density which have become known as coronal holes. Figure 1 shows a Mg X λ 625 spectroheliogram of a 5 arc minute x 2 arc minute area centered at the north pole. The pictures, which were made with different exposure times, were constructed from digital data using the Harvard Solar Image Display System. We have designated as NP1 the polar plume in the center of the picture and the plume on the left as NP2. The latter plume appears to lie over an EUV bright point located at a latitude of about 83° on the hemisphere of the sun facing the earth. It appears that most, perhaps all, EUV polar plumes are rooted in EUV bright points (cf. Bohlin, et al., 1975a, 1975b). EUV bright points, which are also prominent in X-ray photographs, are associated with small bipolar magnetic regions (cf. Golub, et al., 1974, 1976).

Three particularly well observed plumes were selected for analysis, the plumes NP 1 and NP 2 mentioned above and another plume, designated NP 1*, observed in the same location as NP 1 eight hours later. NP 1* may or may not be the same feature as NP 1. Spectroheliograms were obtained simultaneously in the spectral lines Ly α λ 1216, C II λ 1335, C III λ 977, O IV λ 554, O VI λ 1032, and Mg X λ 625. The plumes were visible only in

the latter two lines, which were used in the analysis described below. Data from 10 O VI and 10 Mg X spectroheliograms were utilized for the study of NP1 and NP2 while 6 spectroheliograms in each of these lines were utilized for NP 1*. The individual spectroheliograms were summed in various combinations in order to avoid complications due to time evolution and to superimposed emission or absorption caused by macrospicules (cf. Withbroe, et al., 1976). Between the plumes can be seen emission due to various possible sources which we lump together and call the "background". The background consists of radiation from the quiet sun fore and aft of the polar coronal hole, from fainter plumes in the hole and from interplume material. This background was determined for the interstices between plumes and subtracted from the plume emission.

3. Temperature Analysis

The intensity of an EUV emission line is given by the relation (cf. Withbroe, 1970)

$$I = 1.73 \times 10^{-16} A f \int_{-\infty}^{\infty} g G(T) N_e^2 d\ell \quad (1)$$

where I is measured in $\text{erg cm}^{-2} \text{sec}^{-1} \text{sterad}^{-1}$, A is the chemical abundance relative to hydrogen of the element forming the line, f is the oscillator strength, g is the Gaunt factor, $G(T)$ is a temperature dependent term depending on the excitation and ionization properties of the atom producing the line and ℓ is the path length along the line of sight. Equation (1) assumes that the line emission results from collisional excitation by electrons. For O VI λ 1032 there is also a contribution by resonance scattering of radiation from the chromospheric-coronal transition region. However, since the effects of resonance scattering do not affect our results substantially, we defer

discussion of these effects until section 5. Equation (1) also assumes ionization equilibrium. Effects arising from plasma outflow will also be discussed in §5.

If we assume that the gas along the line of sight is isothermal, the ratio of the intensities of the Mg X $\lambda 625$ and O VI $\lambda 1032$ lines will be (cf. Equation (1)).

$$\frac{I_{\text{Mg X}}}{I_{\text{O VI}}} = \frac{(AfgG(T))_{\lambda 625}}{(AfgG(T))_{\lambda 1032}} . \quad (2)$$

Because of differences between the temperature dependence of the functions $gG(T)$ for Mg X $\lambda 625$ and O VI $\lambda 1032$, the ratio of these lines is temperature sensitive (cf. Mariska and Withbroe 1975). Hence, a comparison of theoretical and observed intensity ratios provides a measure of the temperature of the plume under the assumption that the plume is isothermal. That assumption is consistent with the observed behavior of the Mg X/O VI ratio illustrated in Figure 2, which appears to remain constant across the plume within the errors of measurement. In evaluating the theoretical ratios we assumed $\log A_{\text{O}} = 8.6$ and $\log A_{\text{Mg}} = 7.5$ (on a scale where $\log A_{\text{H}} = 12.0$), the oscillator strengths given by Wiese, *et al.* (1966, 1969), and functions $gG(T)$ based on the Gaunt factors of Bely (1966) and ionization equilibrium calculations of Allen and Dupree (1969) and Dupree and Wood (1969).

The observed ratios $I_{\text{Mg X}}/I_{\text{O VI}}$ in the plumes vary from about 0.3 at 30 arc seconds above the limb to about 0.8 between 100 and 125 arc seconds above the limb, significantly below the value of 1.0 obtained for the quiet sun at similar heights by Mariska and Withbroe (1975). This means that plumes must contain cooler material than the

corona in the quiet sun.

Figure 3 gives plume temperatures as a function of inverse radial distance, $S = R_0/R$ where R_0 is the radius of the sun and R is the distance from sun center to a point in the plume. As a first approximation the plume temperatures appear to increase linearly with decreasing S . The mean slope derived from measurements of the three plumes is $dT/dS = -1.6 \times 10^6$ K. The mean temperature of all three plumes for the range of heights observed is $T = 1.1 \times 10^6$ K. This compares favorably with the value of 1.2×10^6 K derived by Saito (1965) under the assumption that white light plumes are isothermal and in hydrostatic equilibrium. It also falls within the range of temperatures, 0.7 to 1.2×10^6 K, inferred by Bohlin et al., (1975a, 1975b) from the presence or absence of polar plumes in spectroheliograms of various lines found between 250 and 610 Å.

4. Density Analysis

For simplicity we assumed a cylindrical model in which the electron density decreased exponentially with distance r from the axis of the cylinder,

$$N_e(R,r) = N_0(R) \exp\left[-\left(\frac{r}{\beta}\right)^2\right], \quad (3)$$

where $N_0(R)$ is the density at the axis at a distance R from the center of the sun. The parameter β provides a measurement of the effective width of the plume. An expression analogous to Equation 3 was used by Saito (1958) to study the variation of surface brightness across plumes observed in white light. An alternate relationship between the electron density and r is the one used by Newkirk and Harvey (1968),

$$N_e(r) = N_0 \left(\frac{d-r}{d}\right)^{1.6}, \quad (4)$$

where d is the radius of the plume. Intensities computed with this relationship were found to fit the EUV data nearly as well as the exponential relationship. From the earth one measures the EUV intensity as a function of distance ρ from the central axis of the plume. From Equations (1) and (3) and the geometrical relationship between ρ and r we obtain

$$I(R, \rho) = 3.46 \times 10^{-16} A_f \langle gG(T) \rangle N_o^2(R) \int_{\rho}^{\infty} \frac{\exp(-2(\frac{r}{\beta})^2) r dr}{\sqrt{r^2 - \rho^2}} \quad (5)$$

This equation assumes that the temperature in the plume does not vary across the width of the plume, an assumption consistent with the observed behavior of the Mg X/O VI ratio (see §3).

Figure 4 gives the parameter β as a function of distance above the limb. These widths were determined from the Mg X measurements. The widths obtained from the O VI data are identical to within the errors of the determinations. The uncertainty in the widths is about 2500 km. A least squares straight line has been fit to the data for the two plumes, NP1 and NP2. Both lines have the same slope and indicate that the plume widths increase with height. Since the widths measured for NP1* have such large scatter, we did not fit a least squares line to them. The overall trend suggests that the width of this plume also increases with height if the discrepant point at $1.07 R_{\odot}$ is ignored. The widths for NP 1* are less reliable than those for NP1 and NP2 due to the low contrast between the intensity of this plume and the background which makes it difficult to reliably determine the variation of intensity across the plume.

The increase in width as a function of height for these EUV plumes is significantly larger than expected on the basis of Saito's (1965) results for white light plumes observed in the 1962 New Guinea eclipse.

Linear extrapolation of his results for $1.12 R_{\odot} \leq R \leq 1.4 R_{\odot}$ to lower heights leads one to expect that β would increase only slightly between $R = 1.0 R_{\odot}$ and $R = 1.1 R_{\odot}$, from about 2.7×10^4 km to 2.8×10^4 km. Because of the small number of EUV plumes studied, and because of the uncertainty of the legitimacy of extrapolating the white light results, we are unable to conclude if this difference is significant. The widths of our plumes are in good agreement with those of XUV plumes measured by Bohlin, *et al.* (1975a, 1975b) who obtained a mean width corresponding to $\beta = 3.2 \pm 0.8 \times 10^4$ km at a radial distance of $1.1 R_{\odot}$. Newkirk and Harvey (1968) obtained a similar result for white light plumes observed in eclipses of 1962, 1963, and 1965, a mean width corresponding to $\beta = 3.1 \pm 1.0 \times 10^4$ km for $R = 1.14 R_{\odot}$.

Figure 5 illustrates for three heights the fit of the theoretical Mg X intensities (curves) calculated from Equation (5) and the parameter β obtained from the mean relationship between β and R as given in Figure 4. For each theoretical curve an appropriate amount of background intensity has been added to the intensity contributed by the plume.

Through use of the widths β determined from the straight line fit to the data in Figure 4, the mean variation of temperature with height obtained from Figure 3, the measured central intensities of the plumes and equation (5), the central densities $N_{\odot}(R)$ were determined as a function of R for each of the three plumes. The results are plotted in Figure 6. For comparison we have also plotted (dashed line) Saito's (1965) densities shifted downward by 0.08 dex to obtain a better fit to our results. His values, which were derived from white light plumes observed in 1962, are

in good agreement with ours, although there is a small difference in density gradient and in absolute scale.

The solid line plotted in Figure 6 gives the variation of density with height at the plume axis predicted under the assumption that the plume is in hydrostatic equilibrium. One can show that if dT/dS is constant, then the equation of hydrostatic equilibrium yields the relation,

$$\ln N_0(S) / N_0(S_0) = \left(1 - \frac{GM_0 \mu M_H}{kR_0 \langle dT/dS \rangle}\right) \ln(T_0/T), \quad (6)$$

where N_0 is the density at the axis of the plume, μ is the mean molecular weight (assumed to be 0.62), T_0 is the temperature at reference height S_0 and the other parameters have then usual definitions. The solid line in Figure 6 was calculated from this equation and the derived relation between S and T (see Figure 3). Within the errors the data are consistent with the assumption of hydrostatic equilibrium over most of the observed height range. There is a slight departure of the densities for NP1 and NP2 from the hydrostatic equilibrium line, the significance of which will be discussed in the next paragraph.

If the plume is to be in hydrostatic equilibrium away from the plume axis, then the plume must be threaded by magnetic field lines that diverge from the plume axis with increasing height in the plume. Along each field line the ratio of the densities at two heights in the plume must be the same as the corresponding ratio along the plume axis. This implies (cf. equation (3)) that the field lines at a height corresponding to $S_2 = R_0/R_2$ will be a factor of $\beta(S_2) / \beta(S_1)$ further away from the plume axis than they are at a height corresponding to $S_1 = R_0/R_1$.

We wish to investigate the significance of the apparent departure of NP1 and NP2 from hydrostatic equilibrium. We shall make a hydrodynamic

analysis of NP1, since it is the better observed of the two plumes. As in Saito's (1965) hydrodynamic analysis of the white light plumes, we employ the momentum equation,

$$v \frac{dv}{dR} = \frac{kT}{\langle m \rangle} \left(\frac{d \ln N}{dR} + \frac{d \ln T}{dR} \right) - \frac{GM_{\odot}}{R^2}, \quad (7)$$

where $\langle m \rangle$ is the mean particle mass, which we estimate to be 1.02×10^{-24} gms, appropriate to a fully ionized plasma, 90% H and 10% He by number. We write the continuity equation in the form,

$$\frac{d \ln v}{dR} = \frac{d \ln (1/N_0 \beta^2)}{dR} \equiv X(R), \quad (8)$$

where X may be determined from the information in Figs. 5 and 6.

Substituting equation (8) into equation (7) we have

$$v^2 = - \frac{kT}{\langle m \rangle} \left(\frac{d \ln N}{dR} + \frac{d \ln T}{dR} \right) - \frac{GM_{\odot}}{XR^2}. \quad (9)$$

Assuming NP1 is in the plane of the sky we have at $R = 1.06 R_{\odot}$,
 $T = 1.03 \pm .03 \times 10^6$ oK, $d \ln T/dR = 2.1 \pm .3 \times 10^{-11}$ cm⁻¹, $d \ln N/dR = 2.12 \pm .1 \times 10^{-10}$ cm⁻¹, and $X = 1.28 \pm .16 \times 10^{-10}$ cm⁻¹. Then the most probable value for v is 41 km/s. Using the 1σ extrema for the parameters quoted above, we get lower and upper limits for v of 0 km/s and 65 km/s respectively. A qualitatively similar case may be made for NP2. NP1* seems most consistent with hydrostatic equilibrium, but it has the worst scatter and carries the least weight. We conclude that while the observations are consistent with hydrostatic equilibrium within the errors of the analysis, they are in better agreement with a picture in which high velocity outflow is taking place. The effects of rapid outflow on the assumption of ionization equilibrium is considered in §5. From the integral of equation

(8) we can calculate the relative velocity through the region observed. We find that the velocity at $R = 1.12 R_{\odot}$ is about 35% greater than that at $1.06 R_{\odot}$ while the velocity at $R = 1.02 R_{\odot}$ is about 15% lower.

On the basis of the plume models derived in this investigation, it appears that plumes can contain a significant fraction of the total coronal material in a polar coronal hole. The density along the axis of a plume appears to be about a factor of about 3 higher than in typical polar hole models (Mariska 1976, Munro 1976). If one assumes our plume model is representative of an average plume and that the number of plumes in a polar hole is equal to the number of coronal bright points found there (cf. Golub *et al.* 1974, 1976), plumes will cover about 10% of the area in a polar coronal hole and contain about 15% of the mass. We assume here that all coronal bright points in polar holes are associated with polar plumes, a hypothesis that appears to be consistent with the observations, as was mentioned earlier.

5. Effects of Resonance Scattering and Departures from Ionization Equilibrium

Noyes (1976) has found that resonance scattering of O VI $\lambda 1032$ radiation from the transition layer can contribute a significant fraction of the radiation emitted by coronal material. We evaluated the effect of omitting the influence of resonance scattering on the analysis of plume observations and found that the plume temperatures, temperature gradients, densities, and widths (β) change by about 10% or less when resonance scattering is taken into account. If the plume plasma is in motion, the effects are even smaller because the coronal line profile is Doppler shifted with respect to the wavelength of the transition region line radiation. Since the magnitude of the flow velocities are uncertain and because the parameters derived for our plume model are uncertain by approximately 10% due

to uncertainties in instrumental calibration, ionization equilibrium calculations, and the simplified plume model, etc., introduction of the effects of resonance scattering would not substantially improve the reliability of the plume model. Therefore, in the interest of simplicity, we have omitted the effects of resonance scattering in deriving the models.

If material is flowing out at rapid velocities, departures from ionization equilibrium may be significant (see, e.g., Tworkowski 1975). The character of such departures is not well enough understood at present to make quantitative predictions, but since the velocities would be increasing with height (see §4), we may say qualitatively that the effect is that the kinetic temperature will exceed the ionization temperature by an amount increasing with height in the low corona. In that case the absolute temperatures and the temperature gradient will be larger than derived in the present work.

6. Conclusions

Plumes are an important source of coronal emission in polar coronal holes. The plumes studied here have a vertical temperature gradient $dT/dS \approx -1.6 \times 10^6 \text{ K}$, and an absolute temperature of about $1.1 \times 10^6 \text{ K}$. The density distribution across the plume appears Gaussian, but it is also consistent with near - Gaussian distributions previously used to interpret some white light observations. The density at plume center falls off with a logarithmic gradient slightly steeper than that observed at higher altitudes in white light. The possibility that the plasma is in hydrostatic equilibrium cannot be ruled out, but flow velocities of the order of several times 10 km/sec are in as good, if not better, agreement with the data. Various parameters

we have obtained may be modified up to 10% by a correction for the effects of resonant scattering of the O VI line, but our general conclusions stand. It appears that polar plumes may contain about 15% of the mass in a typical polar coronal hole and occupy 10% of the volume.

ACKNOWLEDGEMENTS

We are grateful to J.D. Bohlin for some stimulating conversations. We thank H. Wadzinski for his help with the computer programming and M. Mouris for his assistance with the data analysis. We are particularly grateful to J. Mariska for his part in calculating the effects of resonant scattering. In carrying out this research, the authors have benefitted considerably from their participation in the Skylab Solar Workshop series on Coronal Holes. The Workshops are sponsored by NASA and NSF and are managed by the High Altitude Observatory. This work was supported in part by NASA contract NAS 5-3949 and Air Force Geophysical Laboratories contract F19628-76-C-0281.

- Ahmad, I.A.: 1976, Bull. Amer. Astron. Soc. 8, 325.
- Allen, J.W. and Dupree, A.K.: 1969, Astrophys J. 155, 27.
- Bell, B. and Noci, G.: 1976, J. Geophys. Res., 81, 4508.
- Bely, O.: 1966, Proc. Phys. Soc. 88, 587.
- Bohlin, J.E., Purcell, J.E., Sheeley, N.R. and Tousey, R.: 1975a,
Bull. Amer. Astron. Soc. 7, 356.
- Bohlin, J.D., Sheeley, N.R. and Tousey, R.: 1975b, in M.J. Rycroft
(ed.), Space Research XV, Akademie-Verlag, Berlin, p. 651
- Dupree, A.K. and Wood, A.: 1969, private communication.
- Dziubenko, N.I.: 1957, Soviet Astron. J., 1, 373.
- Golub, L., Krieger, A.S., Silk, J.K., Timothy, A.F. and Vaiana, G.S.:
1974, Astrophys J., 189, 193.
- Golub L., Krieger, A.S. and Vaiana, G.S.: 1976, Solar Phys., 50, 311.
- Krieger, A.S. Timothy, A.F., Vaiana, G.S., Lazarus, A.J. and Sullivan
J.D.: 1974, in C.T. Russell (ed.), Solar Wind Three, p. 132.
- Mariska, J.T.: 1976, Bull. Amer. Astron. Soc. 8, 338.
- Mariska, J.T. and Withbroe, G.L.: 1975, Solar Phys. 44, 55.
- Munro, R.H.: 1976, private communication.
- Neupert, W.M. and Pizzo, V.: 1974, J. Geophys. Res. 79, 3701.
- Newkirk, G., Jr. and Harvey, J.: 1968, Solar Phys. 3, 321.
- Nikolsky, G.M.: 1956, Astron. Zhur. 33, 87.
- Nolte, J.T., Krieger, A.S., Timothy, A.F., Gold, R.E., Roelof, E.C.,
Vaiana, G., Lazarus, A.J., Sullivan, J.D. and McIntosh, P.S.:
1976, Solar Phys. 46, 303
- Noyes, R.W.: 1976, private communication.
- Reeves, E.M. Timothy, J.G. and Huber, M.C.E.: 1977, Applied Optics,
16, 849.

- Saito, K.: 1958, Publ. Astron. Soc. Jap. 10, 49.
- Saito, K.: 1965, Publ. Astron. Soc. Jap. 17, 7.
- Sheeley, N.R. Jr., Harvey, J.W. and Feldman, W.C.: 1976, Solar Phys.,
49, 271.
- Tworowski, A.S.: 1975, Astrophys. Lett. 17, 27.
- Van de Hulst, H.C.: 1950, Bull. Astron. Soc. Neth. 11, 150.
- Wiese, W.L., Smith, M.W. and Glennon, M.: 1966, Atomic Transition
Probabilities, Vol 1, National Bureau of Standards, Washington.
- Wiese, W.L., Smith, M.W. and Miles, B.M.: 1969, Atomic Transition
Probabilities, Vol 2, National Bureau of Standards, Washington.
- Withbroe, G.L.: 1970, Solar Phys., 11, 42.
- Withbroe, G.L., Jaffe, D.T., Foukal, P.V., Huber, M.C.E., Noyes R.W.,
Reeves, E.M., Schmahl, E.J., Timothy, J.G. and Vernazza, J.E.:
1976, Astrophys. J., 203, 528.

LIST OF FIGURE CAPTIONS

Figure 1. Gray scale images of Mg X λ 625 observations of northern polar plumes. NP1 is at center and NP2 to its left. (a) is a short exposure print showing the distinctness of plumes. (b) is a longer exposure print on which the lower density outer regions of the plumes are visible.

Figure 2. Ratio of line intensities across the plume using intensities integrated between 1.06 and $1.09 R_{\odot}$ above the limb. Average values inside and outside the plumes are indicated.

Figure 3. Observed temperatures inferred from Mg X λ 625/0 VI λ 1032 ratio and Allen-Dupree-Wood ionization equilibria. Solid lines are fits of lines of slope $\langle dT/dS \rangle = 1.6 \times 10^6$ to each plume.

Figure 4. Characteristic width of the density distributions as a function of height. Solid lines are straight line fits to NP1 and NP2. The triangles are for plume NP1, circles for NP2 and crosses for NP1*.

Figure 5. Theoretical intensity distribution across a plume in Mg X for a plume with a Gaussian density distribution fit to the observations of NP1 at three heights.

Figure 6. Vertical density distribution at plume center.



(a)



(b)

POLAR PLUMES OBSERVED IN Mg X λ 625

Figure 1.

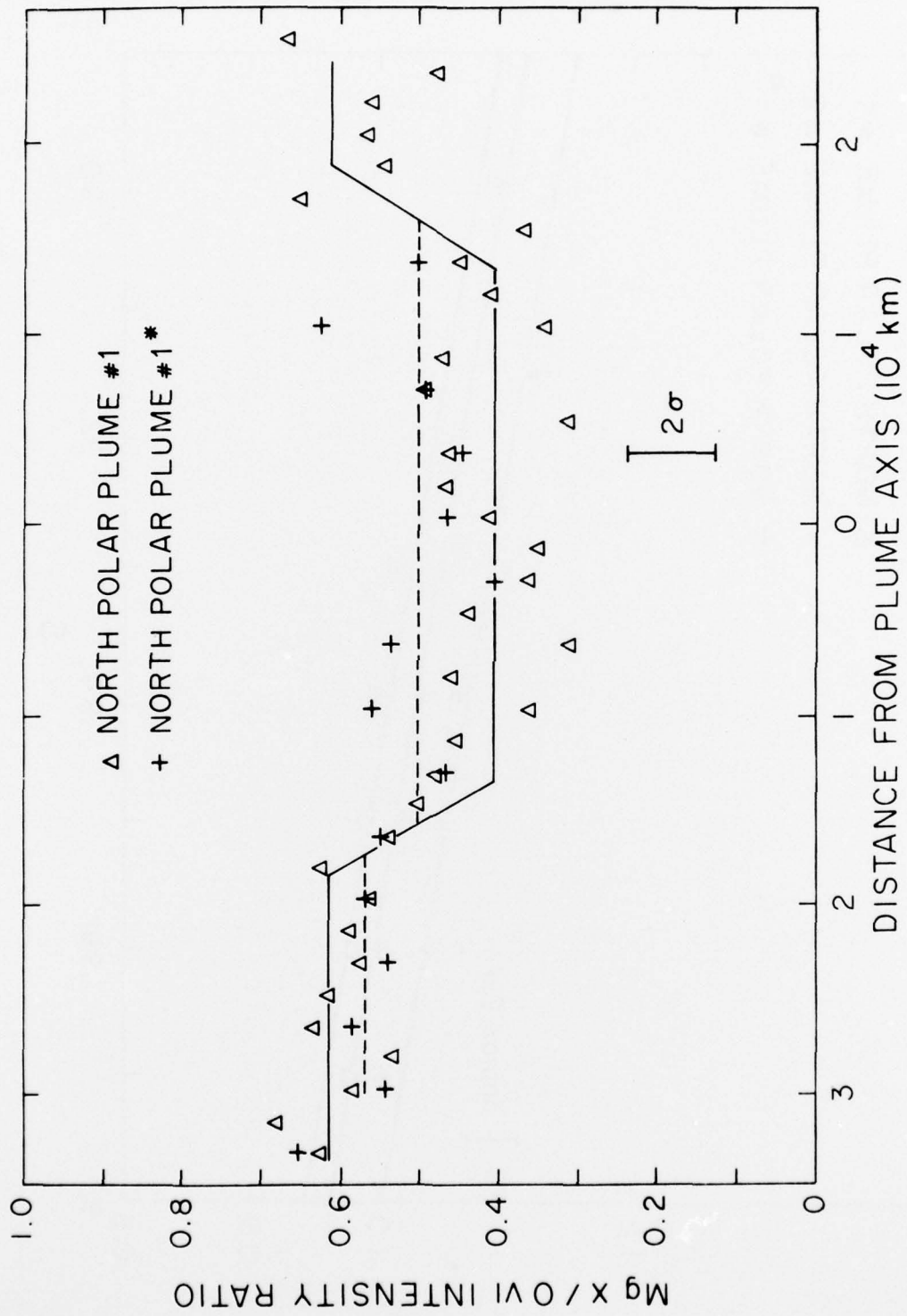


Figure 2.

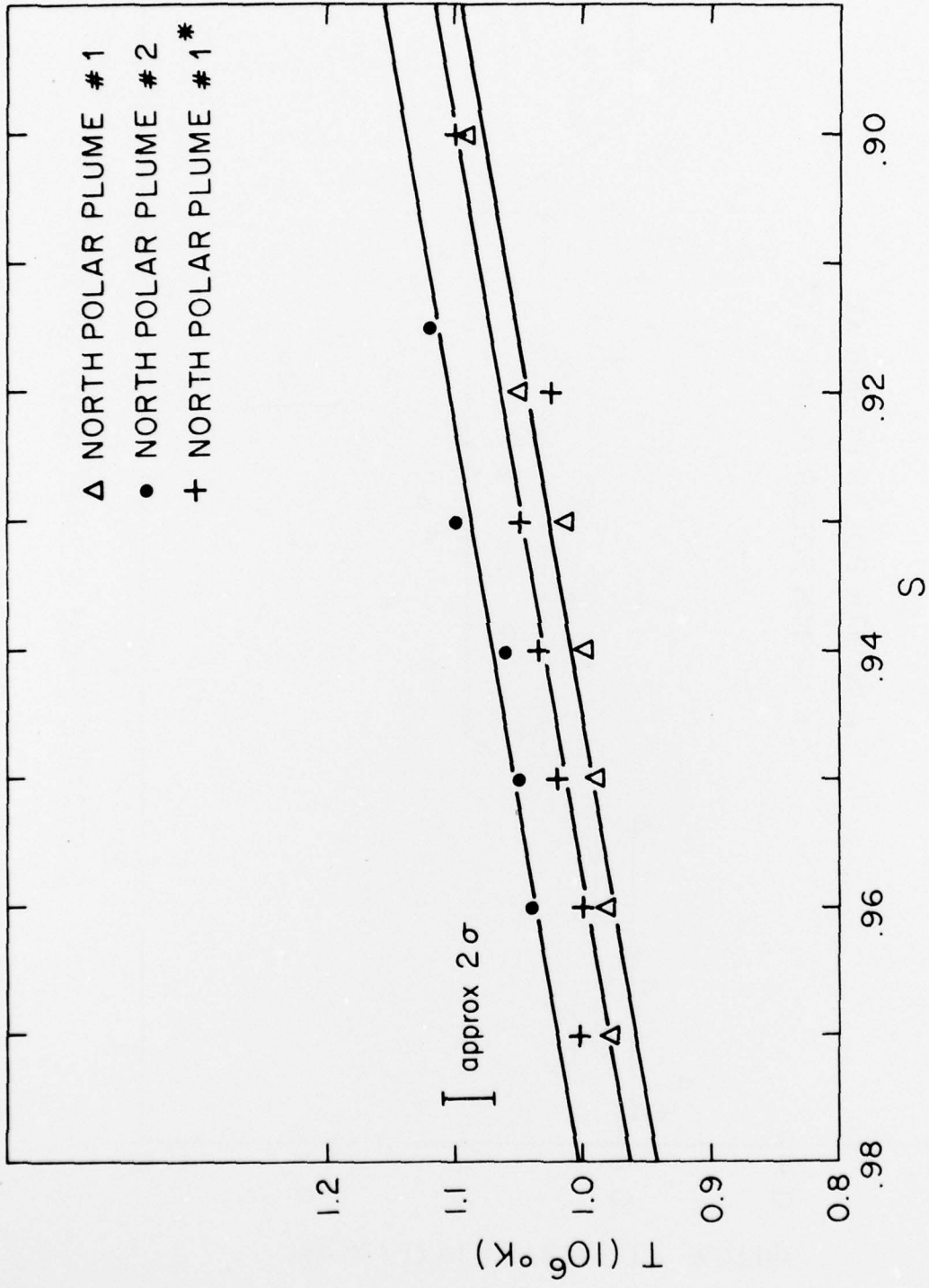


Figure 3.

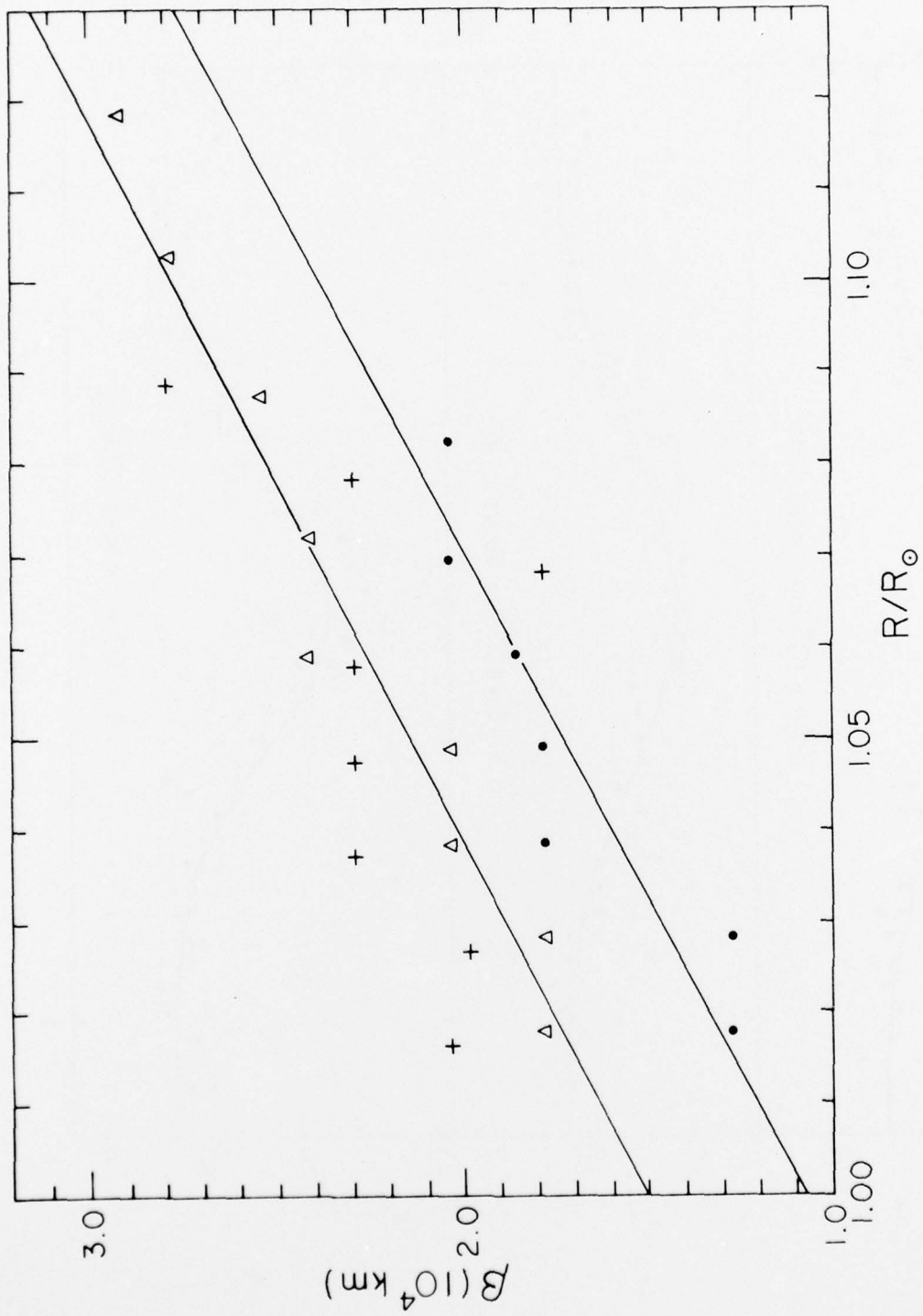


Figure 4.

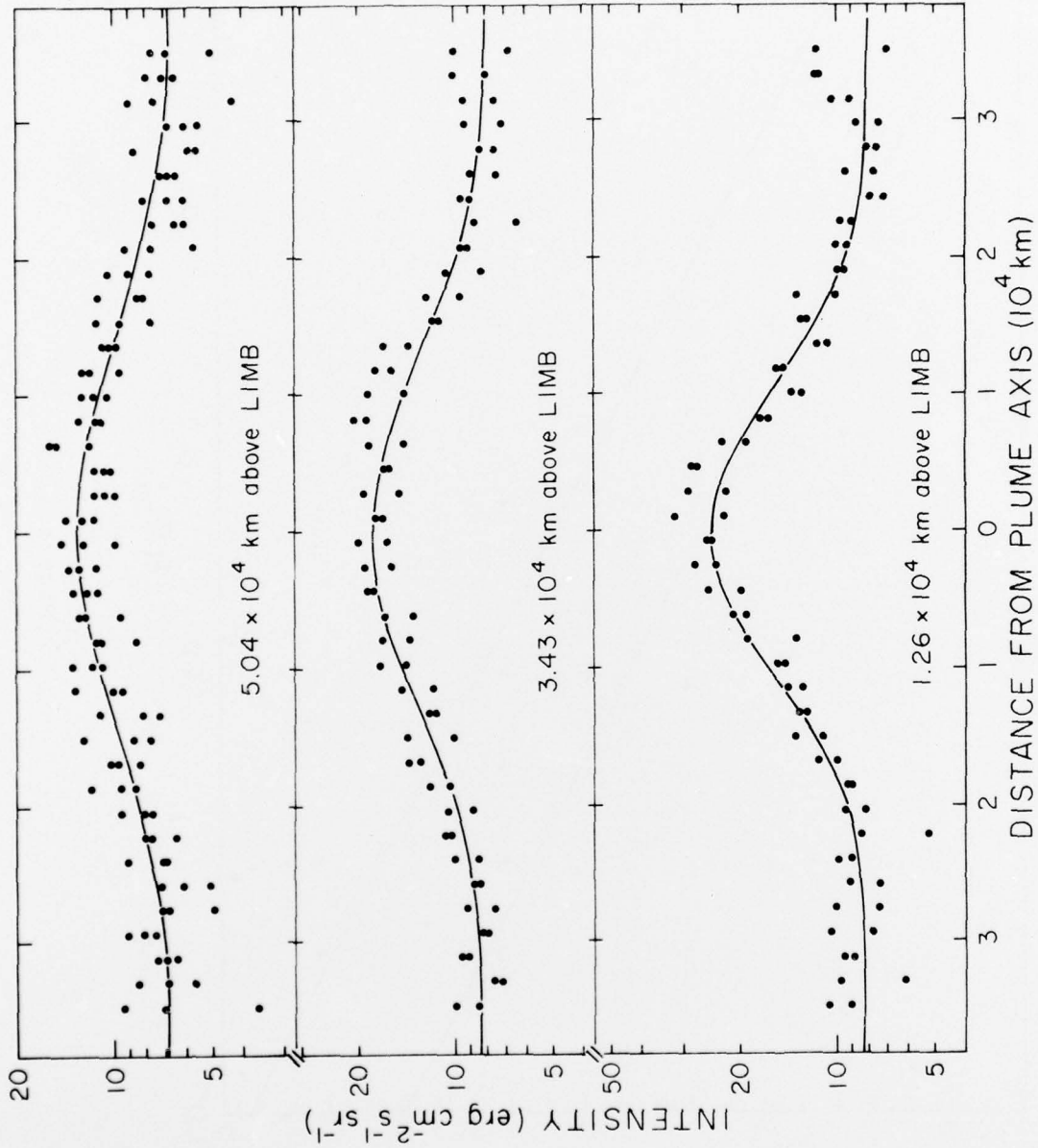


Figure 5.

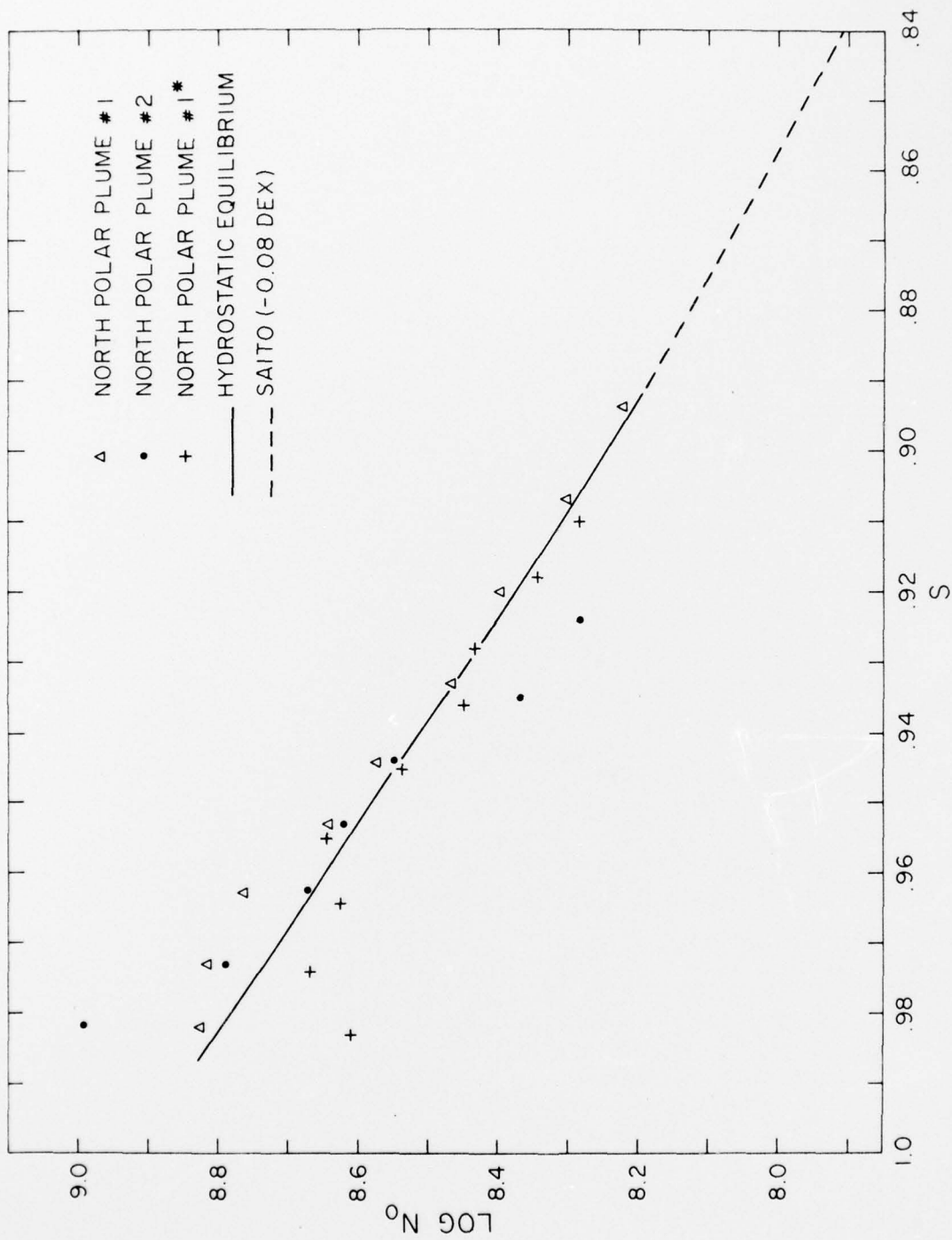


Figure 6.